View metadata, citation and similar papers at core.ac.uk
brought to you by CORE
provided by Universidade do Minho: RepositoriUM

Optical Microtopographic Inspection of Asphalt Pavement Surfaces

Manuel F. M. Costa[a], Freitas E. F. [a] Torres H.[a], Cerezo V.[b]
[a]University of Minho, Campus de Azurém, Guimarães, Portugal;
[b]IFSTTAR, AME-EASE, F - 44344 Bouguenais, France

ABSTRACT

Microtopographic and rugometric characterization of surfaces is routinely and effectively performed non-invasively by a number of different optical methods. Rough surfaces are also inspected using optical profilometers and microtopographer. The characterization of road asphalt pavement surfaces produced in different ways and compositions is fundamental for economical and safety reasons. Having complex structures, including topographically with different ranges of form error and roughness, the inspection of asphalt pavement surfaces is difficult to perform non-invasively. In this communication we will report on the optical non-contact rugometric characterization of the surface of different types of road pavements performed at the Microtopography Laboratory of the Physics Department of the University of Minho.

Keywords: Rugometric characterization, asphalt pavement, microtexture, basalt, granite.

1. INTRODUCTION

One of the most important parameters in road management is skid resistance. Skid resistance of pavements is the friction force developed at the tire-pavement contact area. This force is an essential component of traffic safety because it provides the grip that a tire needs to maintain vehicle control and for stopping in emergency situations [1].

Skid resistance has two major components: adhesion and hysteresis. Adhesion results from the shearing of molecular bonds formed when the tire rubber is pressed into close contact with pavement surface particles. Hysteresis results from energy dissipation when the tire rubber is deformed when passing across the asperities of a rough surface pavement. These two components of skid resistance are related to two key properties of asphaltic pavement surfaces, that is microtexture and macrotexture. Skid resistance changes with traffic loading as a consequence of the wearing effect of the tyres on the surface [1].

While macrotexture is easily and directly acquired using profilometers, even at high speeds, microtexture is difficult to acquire and therefore the micro-roughness of roads' surface was not yet sufficiently studied in order to develop robust skid resistance models. Previous studies indicate that skid resistance could be measured without contact in the future [2, 3]. For exemple, [4] developed a model to predict road surface friction coefficients from only macro and microtexture at all speeds and highlighted the existence of strong effects from both macro and microtexture on road surface frictions. Also, [5] worked on modeling approaches to calculate friction forces from road surface texture by introducing in the models terms related respectively to the macrotexture and the microtexture.

Optical triangulation in different approaches allow the establishment of metrological systems that by its inherent relative simplicity robustness and reliability can cope with most modern requirements of the non-invasive inspection of objects and surfaces both smooth or rough [6]. Among the different optical microtopographers the active triangulation based MICROTOP family of systems [7] was successfully applied to a large number of different samples and metrological tasks including the inspection of the rather rough surface of fracture of granite blocks [8] and other surfaces with complex relief structures.

This paper presents the first stage of a comprehensive research that aims at determining which rugometric parameters are correlated to skid resistance/friction measurements under controlled conditions.

In this stage the rugometric characterization of six asphalt pavement surfaces with different aggregate types, grading and asphalt bitumen was performed and the influence of each one of these factors on rugometric parameters is being analyzed.

2. MATERIALS AND METHODS

2.1 Materials

The materials used for the analysis were asphalt mixtures. Asphalt mixtures are made of aggregates and binder. With the combination of two types of aggregates with different grading, granite and basalt, and two types two types of binder, asphalt bitumen 35/50 and rubberized asphalt, three types of mixtures were produced:
JG – asphalt concrete (35/50 penetration asphalt), granite aggregates;
JB - asphalt concrete (35/50 penetration asphalt), basalt aggregates;
JBB – Gap graded rubberized asphalt (20% rubber by bitumen weight), basalt aggregates;
JBG - Gap graded rubberized asphalt (20% rubber by bitumen weight), granite aggregates;
JDG – drainage asphalt (porous asphalt); (35/50 penetration asphalt), granite aggregates;
JDG – drainage asphalt (porous asphalt); (35/50 penetration asphalt), basalt aggregates.

These asphalt mixtures offer considerably different surface conditions to traffic pass by and have two types of aggregates, granite which is widely used and basalt which is expected to be harder and for that reason more resistant to wear. Also, the existence of rubber in the bitumen is expected to affect the rugometric characteristics of the surface when the pavement is new.

2.2 Sample preparation

The asphalt mixtures were designed to attain the characteristics of the mixtures. Next, 6 slabs were produced in laboratory as shown in Figure 1 a). Each slab was cut into two equal samples of 30×30 cm^2, making a total of 12 samples. In each slab, 9 squares with 1 cm were identified to carry out in that area the microtexture acquisition (Figure 1 b)). Finally, 108 microtexture casts made of silicone were done (Figure 2) to carry out the microtopography measurement.

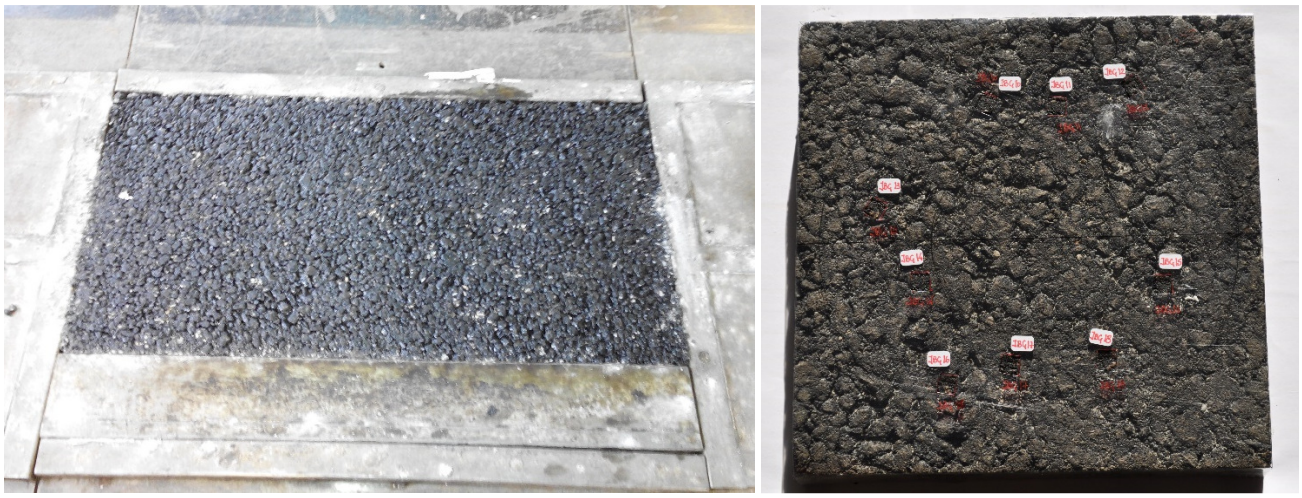

a) b)

Figure 1. Asphalt mixture after compaction and acquisition area identification

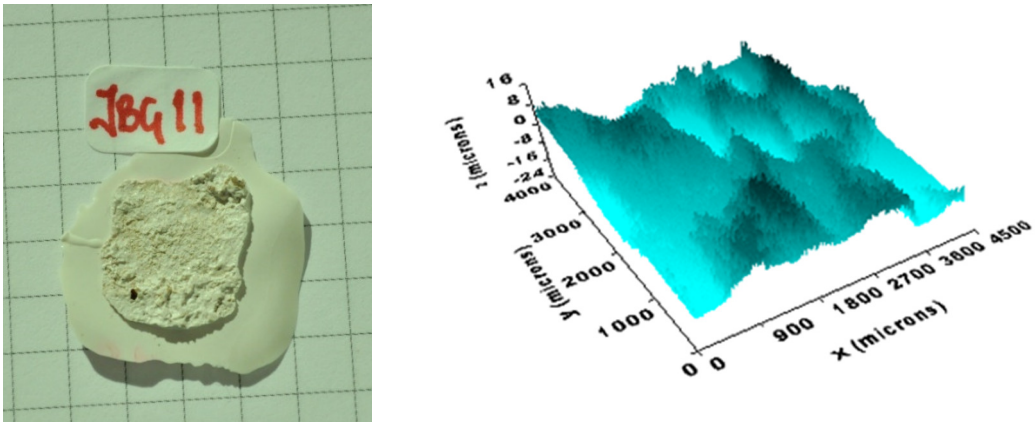

Figure 2. Example of the silicone replica of a section of an asphalt mixture and a partial 3D map.

2.3 Microtexture

For several years optical profilometers and microtopographers were developed at the Physics Department of the Universidade do Minho aiming different applications. For many years the MICROTOP microtopographers (figure 3.) were successfully applied to the inspection of a large range of surface types and inspection tasks with high versatility and reliability, large measuring range, good accuracy and resolution that now can be set from the micrometer range down to the nanometer range [3]. Discreet active triangulation [4] is the method employed. Essentially in this kind of sensors a beam of light shines on the sample at some angle and the reflected light is collected at another angle.

The surface to be inspected is scanned by one oblique light beam. Two HeNe lasers at 632.8 and 534nm, and, one Xe white light sources are available and can be easily interchanged. The incident light is collimated and focused. A small, diffraction limited, bright spot is thus projected onto the sample. The bright spot is imaged both perpendicularly and specularly onto electronic photosensitive detection systems in order to assess its lateral position. The photosensors are one 2048 pixels Fairchild CCD linear array on the specular arm and a Reticon line scan camera. However, one PSD and a differential detector are available and can easily replace the linear arrays. The area of the surface to be inspected is scanned point by point by the "sensor's tip" (the light beam focused onto the surface). The highest system's robustness was sought. Also a high lateral positioning resolution and accuracy should be achieved. Thus both the incidence arm and observation arms of the sensor are kept fixed.

In order to perform the sample's scanning it will be moved by means of a precision XY displacement table driven by precision step motors. Piezo-driven motors allow positioning with nanometer resolution in a 1.5mm range. At each scanning point, on a rectangular array separated by distances down to 1.25 μm, the lateral spot's position in both sensors is obtained and registered. The spot's shift on both detectors' planes, between consecutive scan positions is directly related with the height differences between those surfaces' inspected points. In the "specular" of the system the detector can be positioned (just introducing an adapter) tilted relative to the observation optics in order to increase the depth range of the sensor (Schleimpflug' condition). Employing the linear arrays both arms are on a confocal arrangement allowing the best resolution.

The incidence set-up comprises apart from the light source a neutral density variable filter, a motorized beam steering system, a spatial filter and focusing optics. The change on the incidence angle is made synchronized with the change of the observation angle on the specular arm. A vertical movement precision stage endowed of computer controlled motion provided by a reliable accurate DC encoder with high positioning repeatability and resolution is used refocusing of the observation optical system but especially for calibration of both arms of the sensor. In order to resolve shaded areas and mutual reflections, a high precision rotational stage is used allowing easy change to opposite light incidence. Often the faces of the surface to be analyzed are not parallel or simply the surface to be inspected does not lie horizontally. In order to maintain the best height resolution a tilt table was incorporated to the samples' positioning system. Furthermore it may allow the inspection of 3D objects or surfaces with pronounced holes of it, for instance.

The observation optical systems are formed by microscope objectives chosen according to the characteristics of the surface's relief. In both sensor' arms the objectives can be independently focused. They will be used to image the light spot onto the opto-electronic photosensitive detection systems. Both the "normal" and the "specular" sensors' arms are attached to a XYZ precision displacement table for finer adjustments. A 2D CCD camera was attached to the system allowing the capture of bidimensional colour images of the scanned area for matching and improved visualisation aid. Projection of the actual 2D image onto the 3D map is being studied at the moment. In order to cope with different requirement different photosensitive systems are available and all are interchangeable. A personal microcomputer acquires the data and takes control of the whole inspection process and result's presentation. At the end of the inspection process we may have just one but typically will have two sets of data one for each sensor's arm. Data processing is independently performed and two sets of parameters and functions are obtained by triangulation and scattering analysis. The correlation of the sets of data is investigated. Comparison and matching is performed in order to obtain just one the best set of reliable and accurate data.

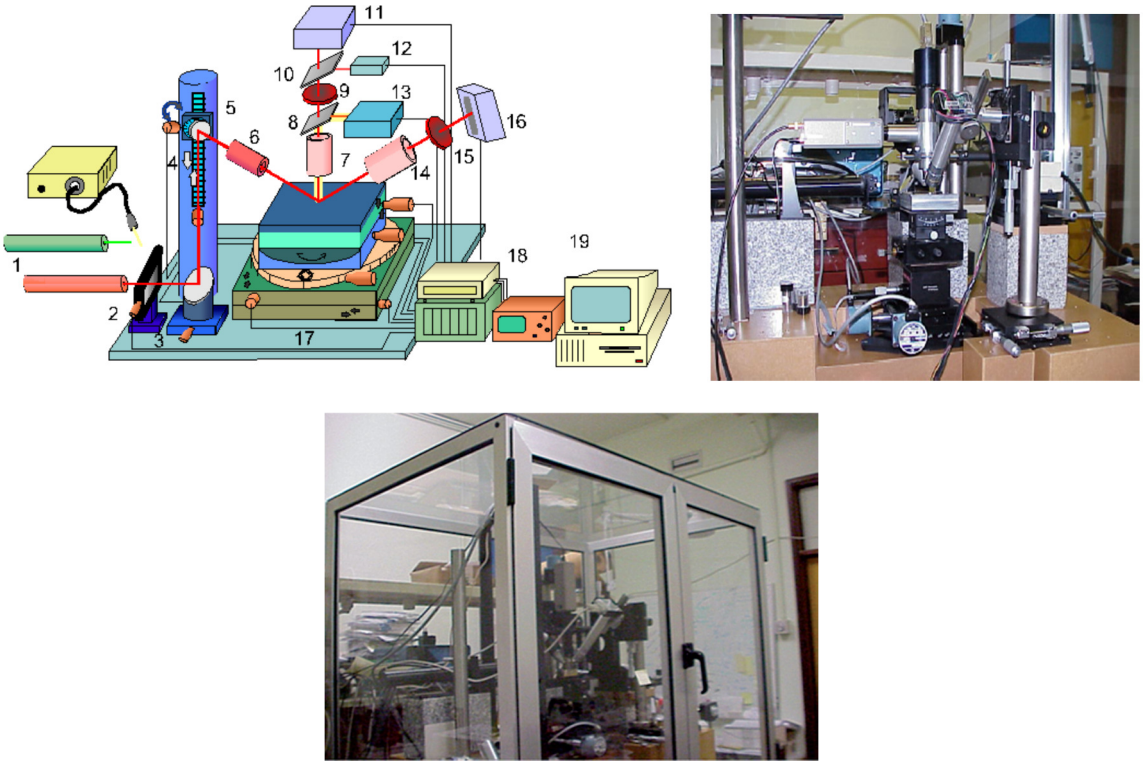

Figure 3. The MICROTOP.06.MFC microtopographer: 1. Interchangeable light sources; 2: Vibration isolation stand; 3. Neutral density filter; 4. Beam steering system; 5. Incidence angle control motorised system; 6. Incidence optics; 7. Normal observation optics; 8. and 9. Beam splitters; 10. Interference filter; 11. Normal photosensitive detection system; 12. Photodetector; 13. Video camera and illuminator; 14. Specular observation optics; 15. Interference filter; 16. Specular photosensitive detection system 17. Sample support and motorised positioning system; 18. Data acquisition and control system; 19. Microcomputer.

3. RESULTS ANALYSIS

The roughness of the 108 silicone surface replicas was measured (table 1). The descriptive statistics of the rugometric parameters Ra, Rq and Rt (ISO 4287 parameters: average roughness, Ra, the root mean square roughness, Rq, and the total roughness, Rt) determined for the 6 pavement surfaces reveal high average differences, nevertheless with a lower significance for Rt (Table 1). In what concerns each one of these parameters, while they show similar minimum values,

maximum values spread over a wider range up to a difference of about 3 times the lowest maximum registered (Figures 4 to 6). Also, the value of the variance is generally higher than the mean, particularly for Rt. Therefore microtexture results are overdispersed.

Table 1. Descriptive statistics of the samples.

Microtexture indicator	parameter	JBB	JB	JBG	JDB	JDG	JG
Ra (µm)	Mean	5.16	7.41	9.28	8.27	4.85	9.61
	Standard deviation	1.93	3.68	4.80	3.56	1.28	2.70
	Maximum	9.90	13.28	19.00	15.72	6.31	13.77
	Minimum	3.07	4.15	2.78	3.70	3.03	3.88
	Variance	3.52	12.49	21.51	11.71	1.49	6.79
Rq (µm)	Mean	6.64	9.64	11.70	10.23	6.21	12.19
	Standard deviation	2.51	4.86	5.97	4.23	1.69	3.46
	Maximum	13.48	17.50	23.23	18.89	8.19	18.23
	Minimum	3.90	4.92	3.61	4.79	4.00	4.76
	Variance	5.94	21.76	33.24	16.52	2.60	11.11
Rt (µm)	Mean	45.89	64.08	67.49	56.91	45.19	71.82
	Standard deviation	14.84	26.38	19.01	20.37	12.80	16.76
	Maximum	84.53	114.21	98.87	91.20	65.57	88.46
	Minimum	22.97	34.72	34.45	27.52	28.93	31.13
	Variance	207.84	642.53	337.18	382.87	148.91	260.85

Through a box and whisker plot, Figures 4 to 6 also show clearly less dispersion on mixtures JBB and JDG for parameters Ra and Rq. Again, Rt has a distinct performance.

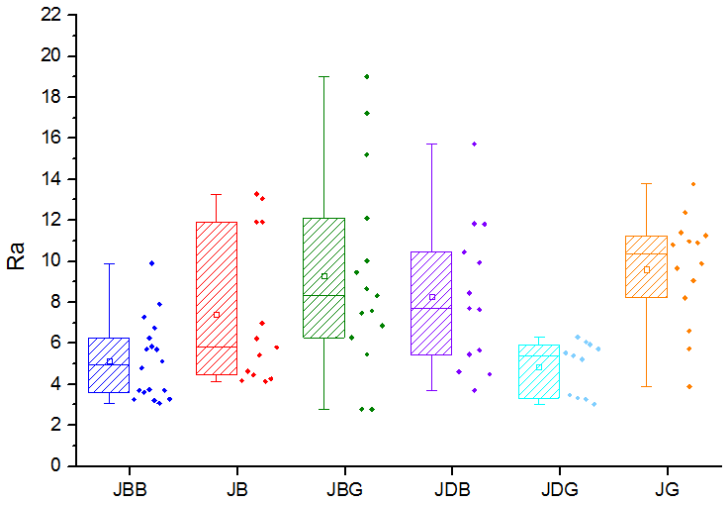

Figure 3. Box and whisker plot of Ra.

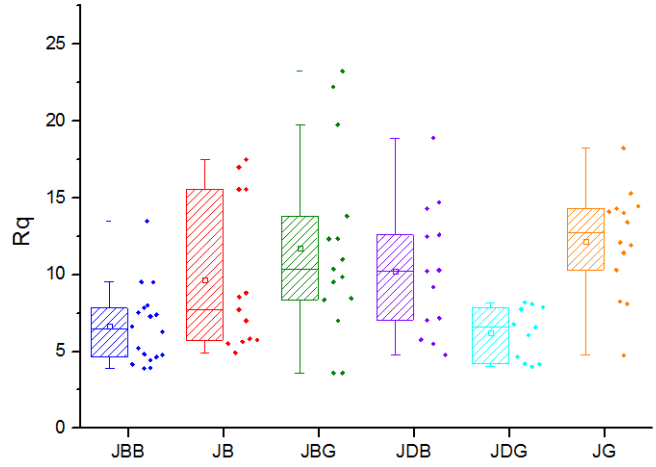

Figure 4. Box and whisker plot of Rq.

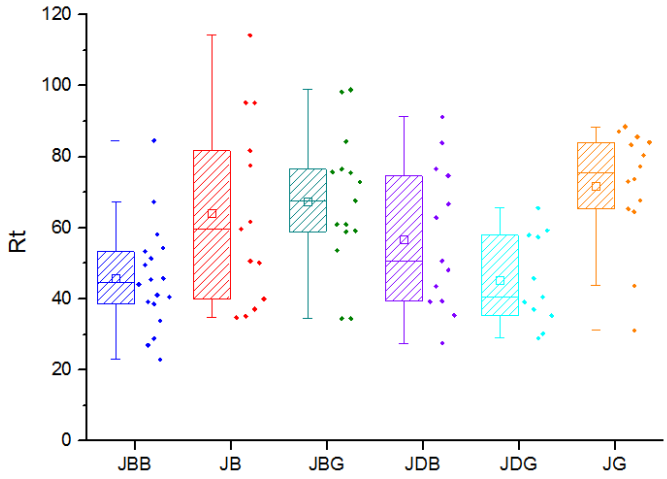

Figure 5. Box and whisker plot of Rt.

3.1 Correlation between parameters

Previous results point to a strong correlation among the rugometric indicators. The values Ra, Rq and Rt were organized in ascending order based on Ra as depicted in Figure 7. Similarity between the behavior of Ra and Rq is clear. The coefficient of determination (R^2) of these parameters is 0,99 while for Rt the R^2 it is much lower, 0,88. Consequently, Ra and Rq follow the same trend and have similar average values and provide similar information when the asphalt mixtures under analysis are coated by asphalt bitumen. Figure 7 indicates, through the random position of the materials, that aggregates size does not affect the values of these rugometric indicators.

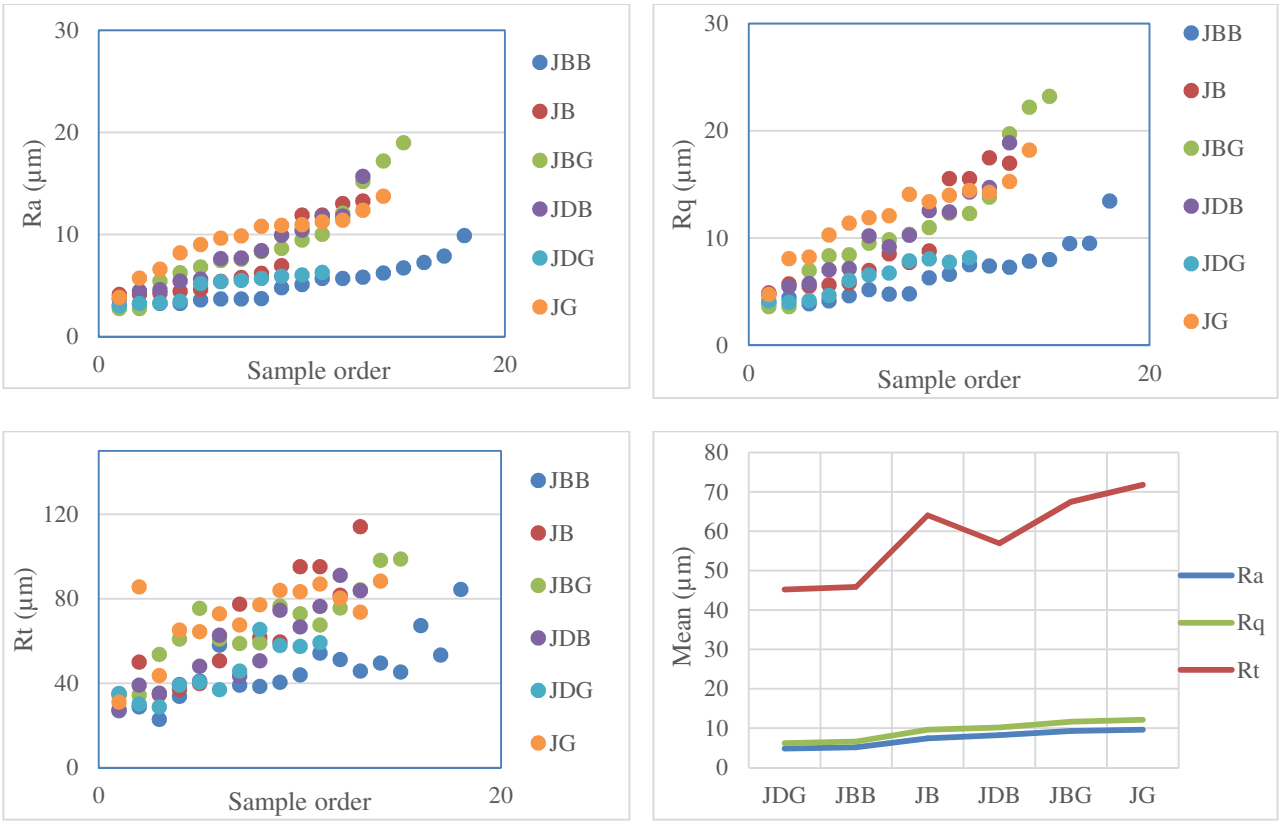

Figure 6. Ra, Rq, Rt determined for each sample and corresponding average values.

3.2 Welch's t-test

The Welch's t-test, or unequal variances t-test, was used to verify if the mean Ra, Rq and Rq values are equal among each material under analysis. This test is more reliable when the-samples have unequal variances and unequal sample sizes as presented in Table 1. The two-tailed p-values from Welch's t-test for parameter Ra, Rq and Rt are presented in Tables 2 to 4, for a significance level of 0,5%. These results are discussed in the following subsections.

Table 2. Two-tailed p-values from Welch's t-test for the parameter Ra.

Pavement	JG	JB	JBG	JBB	JDB	JDG
JG						
JB	0.0919					
JBG	0.8209	0.2537				
JBB	<0.0500	0.0603	<0.0500			
JDB	<0.0500	0.5505	0.5279	<0.0500		
JDG	<0.0500	<0.0500	<0.0500	0.6062	<0.0500	

Table 3. Two-tailed p-values from Welch's t-test for the parameter Rq.

Pavement	JG	JB	JBG	JBB	JDB	JDG
JG						
JB	0.1336					
JBG	0.7887	0.3236				
JBB	<0.0500	0.0572	<0.0500			
JDB	<0.0500	0.7470	0.4531	<0.0500		
JDG	<0.0500	<0.0500	<0.0500	0.5907	<0.0500	

Table 4. Two-tailed p-values from Welch's t-test for the parameter Rt.

Pavement	JG	JB	JBG	JBB	JDB	JDG
JG						
JB	0.3779					
JBG	0.5199	0.7031				
JBB	<0.0500	<0.0500	<0.0500			
JDB	<0.0500	0.4455	0.1697	0.1123		
JDG	<0.0500	<0.0500	<0.0500	0.8945	<0.0500	

3.3 Type of pavement, aggregate and binder effect

From Figure 7 and Tables 2 to 4 it is not possible to see any clear effect of the type of pavement on the roughness parameters considered. The average values for the samples with the same type of mixture are similar only for asphalt concrete. However their variance changes by a factor of approximately 2.

The effect of the aggregate type may be discussed by comparing the mean values for the mixtures with the same aggregate (basalt or granite). The mixtures containing basalt have 2 out of 3 cases similar means and mixtures containing granite have only 1 out of 3 cases similar mean values. Basalt seems to provide more consistent results because granite has at the same time the lowest and the highest mean values of Ra, Rq and Rt.

As a final remark, there is no evidence of the direct effect of the binder used in the preparation of the asphalt samples. Rubberised asphalt (samples JBG and JBB) have significantly different means and the other samples, with conventional bitumen, have 2 cases out of 5 with similar means.

4. CONCLUSION

Optical non-contact rugometric characterization of six asphalt mixtures used in road pavement surfaces was carried out. These mixtures represent the road surface immediately after laid, while the asphalt bitumen coats the aggregates in direct contact with tyres. The rugometric parameters under analysis were the average roughness, Ra, the root mean square roughness Rq and the total roughness Rt.

Based on their descriptive statistics and the comparison of the means the following main conclusion can be drawn:

- About 2/3 of the results are overdispersed, particularly Rt;
- Ra and Rq have a strong correlation providing similar information;
- The type of surface does not affect the rugometric parameters, as expected;
- Basalt mixtures have more consistent results than granite;

- The type of bitumen does not affect directly the rugometric parameters.

Future work will compare the rugometric results before and after wearing of the samples and discuss the effect of the aggregate type and type of asphalt mixture.

ACKNOWLEDGMENTS

This work was partially financed project PEst-OE/ECI/UI4047/2014 supported by Portuguese Foundation for Science and Technology.

REFERENCES

[1] Noyce, D. A., Bahia, H. U., Yambo, J. M., & Kim, G., "Incorporating road safety into pavement management: maximizing asphalt pavement surface friction for road safety improvements", Draft Literature Review and State Surveys, Midwest Regional University Transportation Center (UMTRI), Madison, Wisconsin (2005).

[2] Ueckermann, A., Wang, D., Oeser, M., & Steinauer, B., "A contribution to non-contact skid resistance measurement", International Journal of Pavement Engineering, 16(7), 646-659 (2015).

[3] Kane, M. and Cerezo, V. "A contribution to tire/road friction modeling: From a simplified dynamic frictional contact model to a "Dynamic Friction Tester" model", Wear 342, 163-171 (2015).

[4] Ergun, M., Iyinam S. and A. Iyinam F. "Prediction of road surface friction coefficient using only macro-and microtexture measurements", Journal of transportation engineering 131.4, 311-319, (2005).

[5] Do, M. and Cerezo, V. "Road surface texture and skid resistance", Surface Topography: Metrology and Properties 3.4 (2015).

[6] Costa M.F.C. "Optical triangulation-based microtopographic inspection of surfaces," Sensors 12(4), 4399-4420 (2012).

[7] Costa, M. F. M. "Surface Inspection by an optical triangulation method", Opt. Eng. 35(9), 2743-2747 (1996).

[8] Vasconcelos, G.; Lourenço, P. B.; Costa, M. F.; Mode I fracture surface of granite: Measurements and correlations with mechanical properties, Journal of Materials in Civil Engineering, 2008, vol. 20, nº. 3, pp. 245-254.